

1 Supplementary Material for: “Recent Geodetic Unrest at Santorini Caldera, Greece”

2

3 Andrew V. Newman¹, Stathis Stiros², Lujia Feng^{1,3}, Panos Psimoulis^{2,4}, Fanis Moschas², Yan
4 Jiang⁵, Costas Papazachos⁶, Dimitris Panagiotopoulos⁶, Eleni Karagianni⁶, Domenikos
5 Vamvakaris⁶

6 1. School of Earth and Atmospheric Sciences, Georgia Institute of Technology, 311 Ferst
7 Drive, Atlanta, GA, USA. anewman@gatech.edu

8 2. Department of Civil Engineering, University of Patras, Greece.

9 3. now at: Nanyang Technological University, Earth Observatory of Singapore, 50 Nanyang
10 Avenue, Block N2-01a-15, 639798, Singapore, lfeng@ntu.edu.sg

11 4. now at: Institute of Geodesy and Photogrammetry HPV F 51 Schafmattstrasse, 34 8093
12 Zurich, panagiotis.psimoulis@geod.baud.ethz.ch

13 5. University of Miami, Rosenstiel School of Marine and Atmospheric Sciences, Miami, FL
14 33149, USA

15 6. Geophysical Laboratory, Aristotle University of Thessaloniki, Greece.

16

17 Geophys. Res. Lett., doi:10.1029/2012GL051286, 2012

18

19

20

21 **Survey GPS data collection and Processing:**

22 All campaign GPS measurements are performed using 0.5 m fixed-height spike-mounts, and are
23 leveled using precision machinist levels, in order to that minimize user-error in both vertical and
24 horizontal measurements. During surveys, sites were occupied for 3-day periods, with the
25 exception of the 2011-I survey in which sites were occupied for 2-day periods due to timing
26 constraints.

27 For all GPS data precise point positions are determined at the University of Miami Geodesy Lab
28 using version 6.1 of the OASIS-GIPSY software using *Blewitt's* (2008) Ambizap algorithm to
29 resolve ambiguities, and using NASA- Jet Propulsion Laboratory precision satellite orbits. All
30 solutions are determined in ITRF2008. Such data reduction methods represent the state-of-the-art
31 in precision GPS processing, and require on average a 2-week latency before solutions can be
32 resolved. More rapid, but noisier solutions are also determined using rapid orbit products from
33 JPL. These orbits have about a factor of 2 increase in their rms positions, but are available
34 within 2 days, and are hence more valuable for warning.

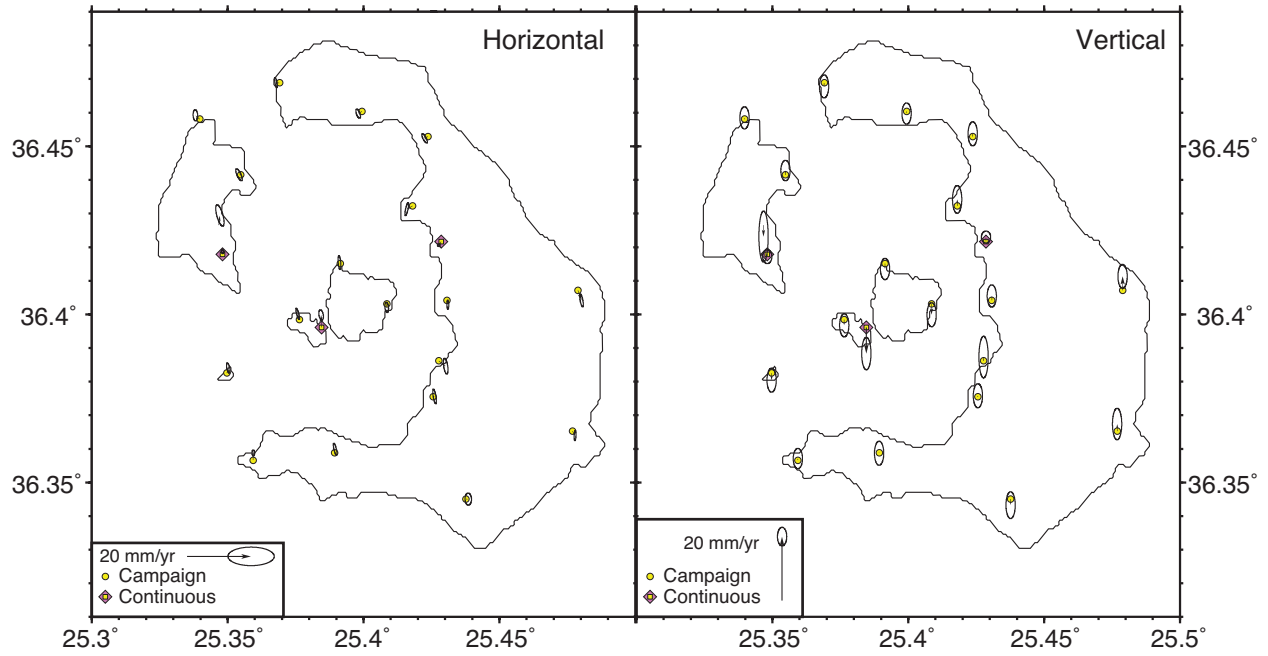
35

36

37 **Additional References:**

38 Blewitt, G. (2008). Fixed point theorems of GPS carrier phase ambiguity resolution and their
39 application to massive network processing: Ambizap. *Journal of Geophysical Research*,
40 113(B12). doi:10.1029/2008JB005736.

2006–2010 GPS Velocities

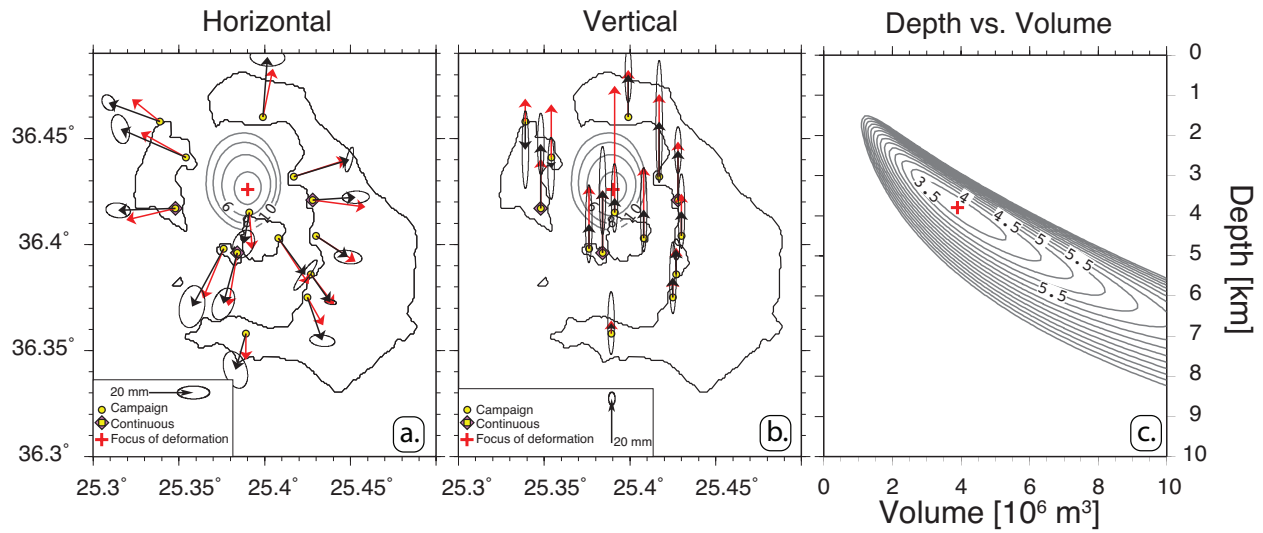


41

42 **Figure S1:** [left] Horizontal and [right] vertical GPS velocity field for Santorini using campaign
43 GPS in 2006, 2008 and 2010, and 3 continuous GPS operating through this time. For all
44 illustrations the mean island velocity (East, North = 7.06, -15.78 mm/yr) as determined by these
45 22 stations is removed. Velocities are scaled to be comparable to other figures in this study.

46

2010-June 2011 Displacements and Model

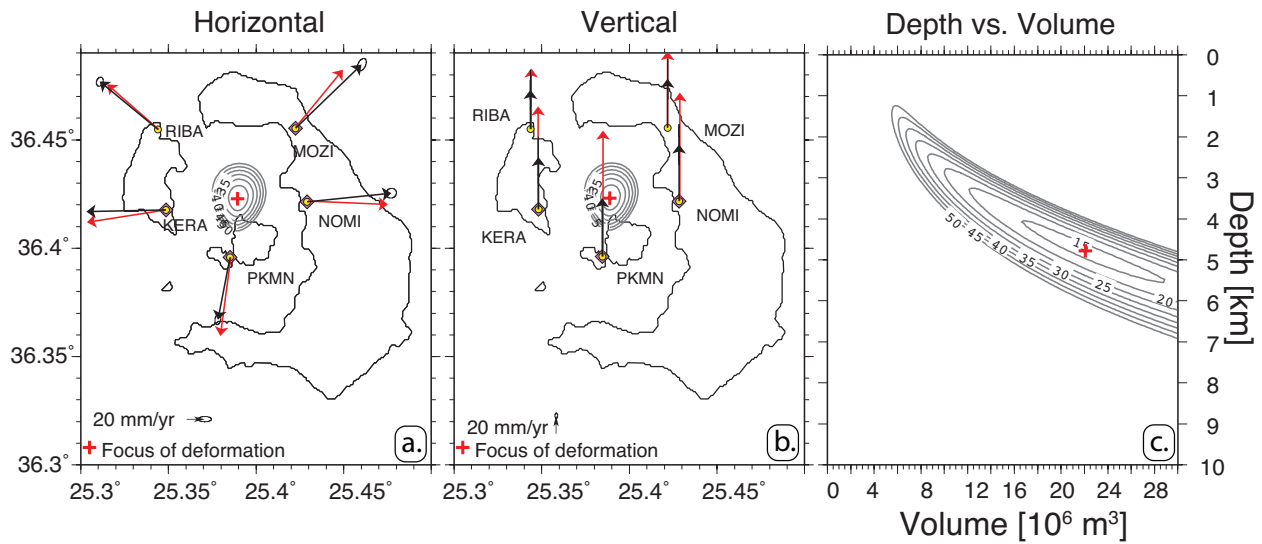


47

48 **Figure S2:** [a] Horizontal and [b] vertical GPS velocity vectors (black arrows) along with model
49 predictions (red arrows) for the best fit spherical source solution (red cross) for the period
50 between the last campaign or continuous GPS data in 2010, and June 2011. [c] Also shown is the
51 depth versus volume trade-off.

52

Sept. 2011 - Jan. 2012 Displacements and Model

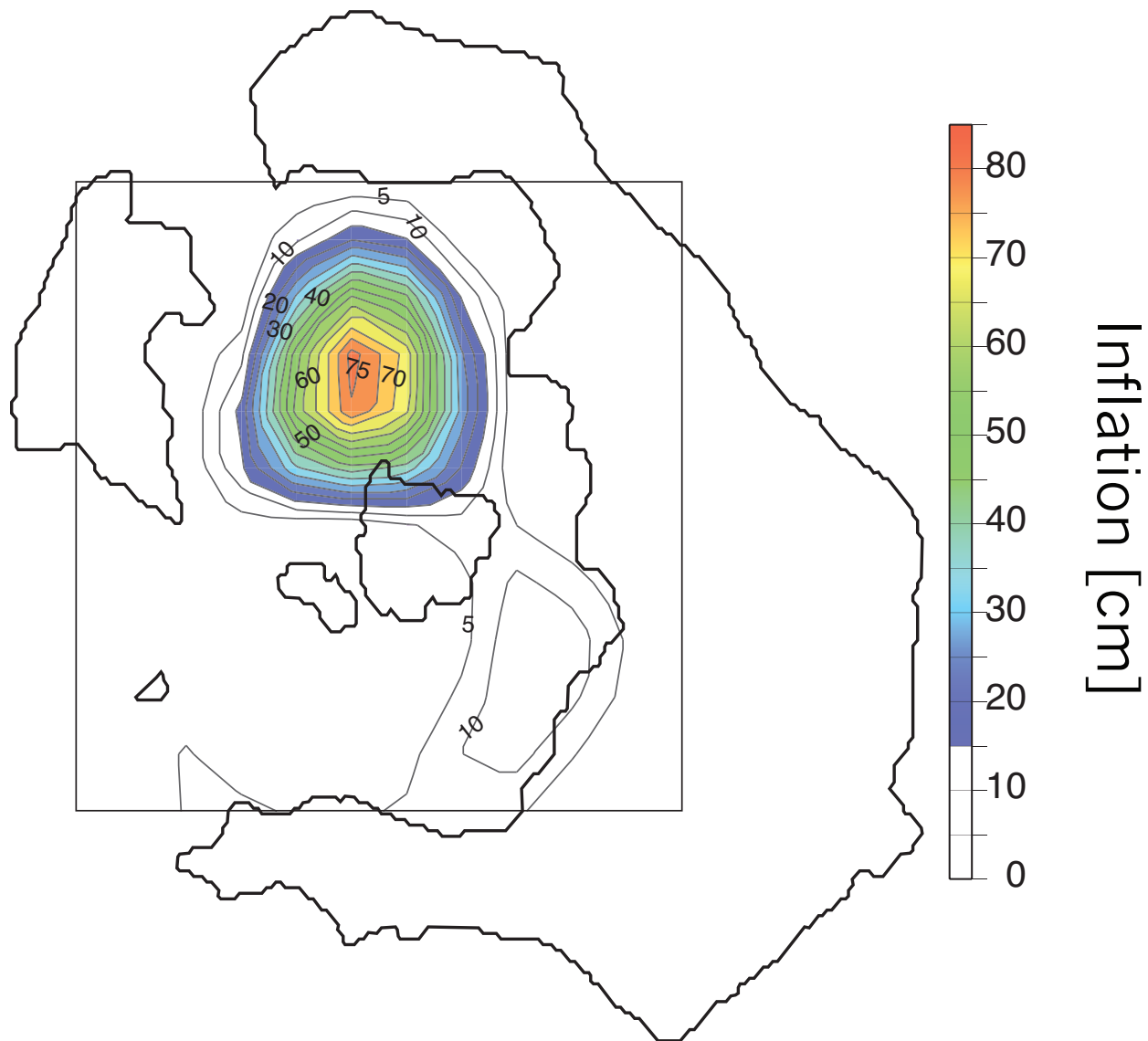


53

54 **Figure S3:** [a] Horizontal and [b] vertical GPS velocity vectors (black arrows) along with model
55 predictions (red arrows) for the best fit spherical source solution (red cross) for the period
56 between September 1, 2011 and January 21, 2012. [c] Also shown is the depth versus volume
57 trade-off.

58

Distributed Sill Source (z=4km)

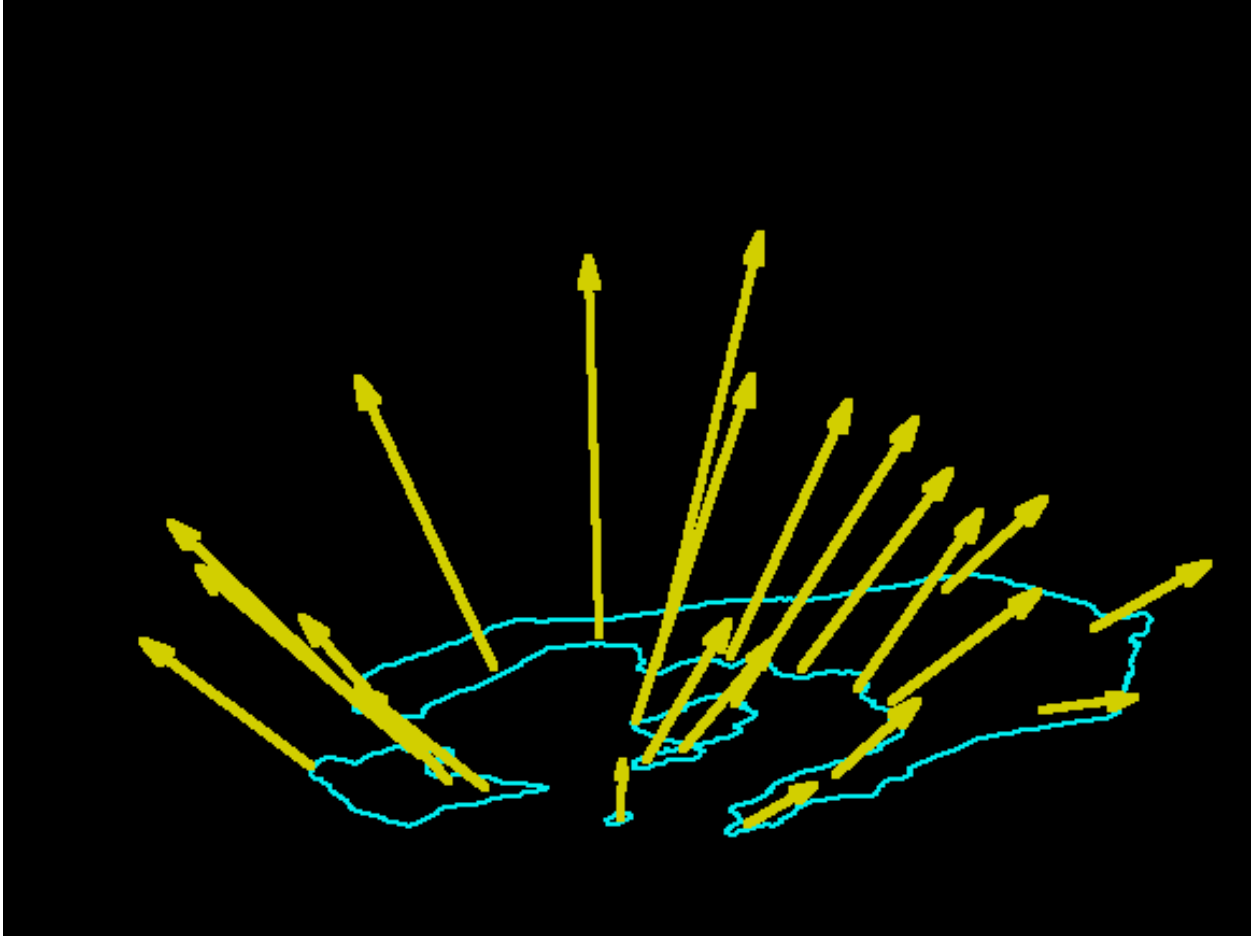


59
60 **Figure S4:** Best fit solution for a distributed sill model for Santorini. This model is fixed at 4 km
61 depth, uses $144 - 0.01^\circ \times 0.01^\circ$ patches to describe opening-mode dislocations following *Okada*
62 [1985]. The solution is smoothed using Laplacian constraint to minimize the reduction in fit
63 quality with model roughness. The model finds a maximum inflation of up to 80 cm in the
64 central caldera, and a volumetric growth of 9.2 million m^3 . While the sill model has about 2x
65 worse misfit (rms = 1.5 cm) than the best spherical source models, the data is useful because it
66 illuminates the potential lateral contribution of inflation.

67

68

69



70

71 **Animation S1:** Three-dimensional animation of the static displacement field between the 2010
72 and September 2011 surveys, corresponding to data shown in Figure 1. Vector magnitudes scale
73 between 1.9 and 7.7 cm, and all radiate from a point in the northern section of the caldera.
74 Animation available at:
75 http://geophysics.eas.gatech.edu/newman/research/papers/Newman_etal_GRL_2012ms01.gif